# Analysis and optimization of one-DOF robotic legs

**Lionel Birglen**
Professor, ASME member
Robotics Laboratory
Department of Mechanical Engineering
Polytechnique Montreal
Montreal, Canada
Email: lionel.birglen@polymtl.ca

**Carlos Ruella***
Graduate Student
Robotics Laboratory
Department of Mechanical Engineering
Polytechnique Montreal
Montreal, Canada
Email: carlos.ruella@polymtl.ca



Almost all walking robots are composed of two or more multi-DOF legs which give them a good ability to traverse obstacles. Nevertheless, their speed and efficiency when traversing rough terrains is, in most cases, arguably limited. Additionally, they have the disadvantage of a generally lower reliability. The design of robust and efficient one-DOF leg is on the other hand a complex process. In this paper, a method to analyze and optimize one-DOF robotic legs is proposed. The results of a virtual simulation are used in combination with some performance indices to optimize the geometric parameters of one-DOF legs. Finally, the results of the simulation and the actual walking performance of a prototype using four legs with the computed optimal parameters are presented and compared with the simulator results. The validation of the simulation model and the optimization method proposed in this paper represents the main contribution of this work.

## 1 Introduction

It is a known fact that wheeled robots are faster and more efficient than legged robots. Nevertheless, traversing difficult and rough terrains constitute their main weakness and the aspect where legged robots excel. Several research initiatives have been led on improving the ability of wheeled robots to traverse obstacles by such diverse means as employing an adaptive suspension system [1], or implementing multi-stage bogie mechanisms [2], etc. As detailed in [3,4], legged locomotion systems are, however, still better at traversing uneven terrains than other locomotion systems.

In the literature, several works dealing with the estimation of the traversability of legged and wheeled robots can be found, as for example in [3, 5–10]. The traversability of a robot is defined as its ability to traverse rough terrains. Several methods to perform a traversability simulation are used. However, the common point of all these works is the need for a model of terrain which the robot should traverse. In robotics, most methods use simple models of terrains composed of a series of panels with random inclination, such as in [5, 9].

Nevertheless, in the field of graphic design most authors agree that fractal methods are the best mathematical representation of realistic terrains. Among the fractal methods available to generate synthetic terrain, the Brownian motion is widely used by graphic designers. This method is generally accepted as being an elegant and simple way to generate artificial terrains [11], but is rarely used in robotics. The only exception to this is by Yokokohji et al. [10] where a method was proposed to generate an uneven terrain using the Brownian motion for later use in a simulation evaluating the traversability of wheeled rovers.

As mentioned before, in order to evaluate the traversability of a mobile robot, it is necessary to specify the terrain that the robot must traverse. The terrain modeling technique used in this work is summarized in Section 2, and presented in more details in [12]. This method generates synthetic landscapes holding similar characteristics to real-life topographies, using as model digital pictures of real

*Address all correspondence related to ASME style format and figures to this author.

terrain profiles.

The simulation algorithm used in this paper analyzes the walk of one leg only, instead of the four or six legs that usually form a legged robot. This simplifies the calculations and drastically reduces the required computation time yet, as will be shown in Section 6, yields surprisingly accurate results. It is indeed assumed that assessing the traversability performance of one leg will provide a general idea of how well a robot composed by several of these legs will perform. Another simplification used here is that the algorithm considers that the terrain is only a 2D profile instead of a 3D surface. Since most of the robotic legs with few DOF have a planar architecture this simplification appeared reasonable. Finally, the terrain is considered solid.

The simulation algorithm proposed here analyzes step-by-step the walking process of a leg to obtain a performance index which estimates the probability of this leg to traverse a specified terrain. The obtained index is later used as the fitness objective function of a multivariable genetic optimization of the geometric parameters defining the leg. Finally, in Section 6, the experimental results of the walking performance of a legged robot build using the optimized leg computed via the proposed method are presented and discussed.

## 2 Synthetic terrain generation

The terrain required for the simulations is produced here using the method proposed in [12]. The latter is based on the principle of Fourier series which reproduce a signal by means of the addition of simple sine functions. Instead of considering the usual time dependent signal of a typical Fourier series, the terrain is regarded as a position dependent signal.

The method aims at producing synthetic terrains with similar geometric characteristics (e.g. smoothness) than those found in Nature. The first step of the method is to take a digital photography of the desired terrain profile with a reference of known size included in the photo (cf. Fig. 1). The reference is placed as closely as possible in the same image plane as the profile itself in order to reduce the errors when the profile in the picture is transformed from pixels into a vector of positions and heights in meters.

Fig. 1. Digital picture of an uneven terrain profile.

Afterwards, the power spectral density of the vector representing the terrain profile is computed. From the latter, the principal harmonics of the terrain profile are extracted, namely each fundamental frequencies $f_n$, with its respective amplitude $A_n$. To generate the synthetic terrain, a simple addition of sine functions with the frequencies and amplitudes extracted from the power spectral density is performed, i.e.:

$$terrain(x) = \sum_{n=1}^{N} A_n \sin\left(f_n x + \Theta_{rand}\right), \qquad (1)$$

where $terrain(x)$ is the height at each point $x$ of the newly generated terrain, and $\Theta_{rand}$ is a randomly generated phase.

Employing this method, a library of different terrains with the same characteristics as the original ones can be produced. In order to generate several terrains, the random phase $\Theta_{rand}$ changed each time. This allows the creation of as much terrains as needed to perform simulations. The number of harmonics used in the terrain reconstruction is chosen by the parameter $N$ in the previous equation. It was empirically noted that using only the first four harmonics the reconstructed terrains resembles closely the real terrains, hence $N$ was set to four. Fig. 2 presents an example of three synthetic terrains produced from the data obtained in Fig. 1.

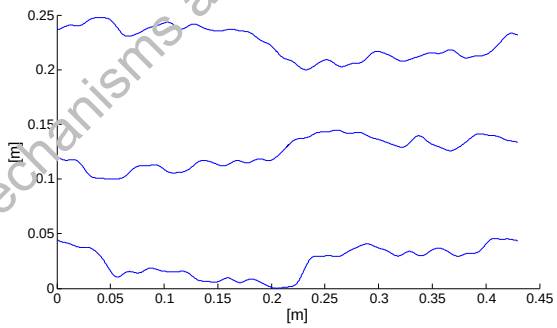


Fig. 2. Sample of three generated synthetic terrain from the same real terrain profile.

## 3 Traversability simulation

In order to evaluate the traversability of one-DOF legs over different types of terrain, the simulation proposed in [12] is used. This algorithm has a modular structure to be able to simulate various mechanical leg architectures crossing over several different types of terrains. The flowchart presented in Fig. 3 summarizes the algorithm of the simulator. It receives as inputs: the geometry of the terrain, the initial position where the leg starts walking, the trajectory of the foot, and the force that the leg is able to apply to the terrain at each point of its trajectory. The traversability simulation was specifically developed for leg architectures with one-DOF. This makes our custom simulator faster and more efficient than commercially available simulators that are designed for general problems.

The trajectory of the foot can be computed by means of the direct kinematics and the force using the principle of virtual work [13] (cf. the example shown in Fig. 4). Note

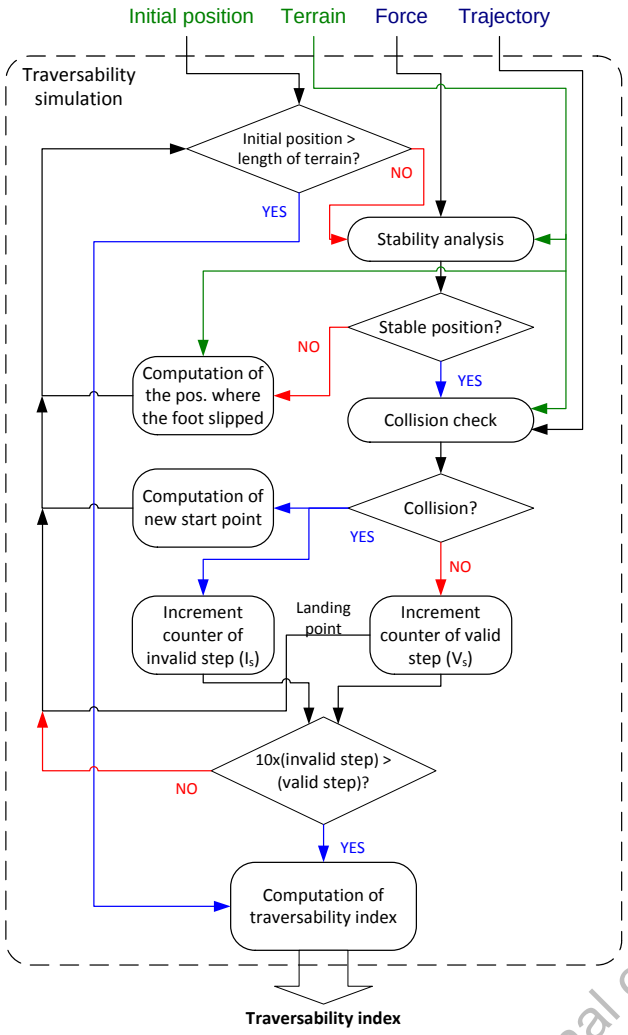


Fig. 3. Flowchart of the proposed algorithm.

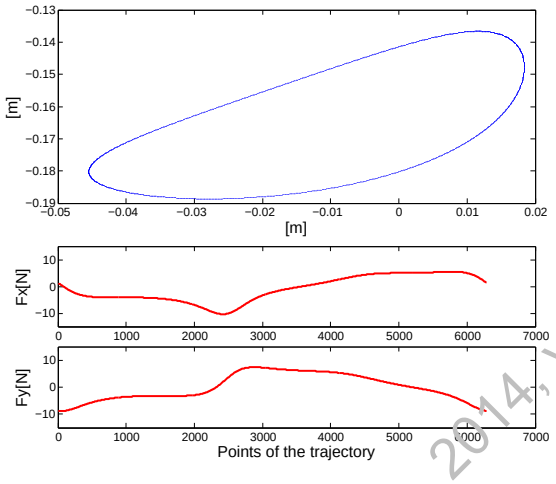


Fig. 4. Example of the trajectory and forces of the foot of a one-DOF leg.

that in the upper part of Fig. 4, the axis correspond to the abscissa and ordinate of the feet position in the same plane of the leg, several definitions are also shown. The step length, for instance, is defined as the distance between the maximal and minimal points in the abscissa of the trajectory. In addition, the trajectory is divided in two phases: the flying phase which corresponds to the part of the trajectory where the foot is moving forwards in the air, and the support phase which is the lower part of the trajectory where the foot is fixed with respect to the terrain and propels the body of the robot forwards.

As illustrated in the flowchart (Fig. 3), the simulation algorithm analyzes each step sequentially from the initial position to the end of the terrain. For every step the leg performs the algorithm checks if the initial position is a stable position. A stable position is defined as any point on the terrain where the foot can be placed without slippage, the Coulomb friction law was used to model the interaction between the foot and the terrain. Then, for the flying phase of the trajectory the algorithm checks if a collision against the terrain occurs. A step where no collision or slippage occurs is considered a valid step. On the other hand, if the initial point is not stable or if the leg collides against the terrain during the flying phase, the step is considered as invalid. This iterative process is repeated until the leg completely traverses the terrain.

Finally, when the simulation is completed, the traversability index ($T_{ind}$) can be computed. This index is a value between zero and one, evaluating the capability of a leg to cross a given terrain. If the simulation give a $T_{ind}$ of zero it means that the leg is not able to cross the terrain. It is also important to mention that if during the simulation the number of invalid steps is ten times the number of valid steps, the simulation stops and $T_{ind}$ is set to zero. When a leg obtains a $T_{ind}$ close to one, this means that it is a suitable leg to traverse that type of terrain. To compute the traversability index, the number of valid and invalid steps is used, namely:

$$T_{ind} = \left(\frac{V_s}{I_s + V_s}\right)\left(\frac{L_t}{(I_s + V_s)\,L_s}\right), \qquad (2)$$

where $V_s$ and $I_s$ are respectively the number of valid and invalid steps, $L_t$ is the length of the terrain and $L_s$ is the length of the step as defined in Fig. 4. The first part of Eq. (2) is a ratio that quantifies the percentage of invalid steps that took place during the simulation. The second factor of the latter equation is an efficiency ratio, which is a key element in the design of any mobile robots. For example, two different sets of geometric parameters for the same leg architecture can produce legs able to successfully traverse the same terrain. Nevertheless, one leg could traverse the terrain in fewer steps than the other. This means that the most efficient leg had fewer collisions and less slippage.

## 4 Optimization of the geometric parameters

In one-DOF robotic legs, the trajectory described by the foot and the force it is able to apply to the terrain depend mainly on the way that the actuator is controlled and the geometric parameters defining its architecture. The actuator can

be appropriately controlled while the robot is walking, but on the other hand, the geometric parameters of the leg once built, are constant. With the aim of developing a robotic leg that does not require a complex control strategy for its actuator, it is desirable to design it with the best possible geometric parameters that will guarantee a good traversability for the robot over a wide variety of terrains.

In the literature, one can find several performance indices used to evaluate legged robots.A summary of the most frequently used indices such as the stability margin, the Froude number, the duty factor and the specific resistance, is reported in [14]. Nevertheless, most of those indices depend on the type of gait and stance that the robot uses to walk. As this paper aimed at optimizing only one leg and not a full walking robot, it was impossible to use most of the commonly documented indices that rely on the gait of the robot. Furthermore, all these indices assume that the robotic leg considered has multiple and independently controlled DOF. This makes it tedious to compare the performances of multi and one-DOF legs. However, for applications where reliability is important, a leg with only one actuator would perform better than a leg with three or four actuators, as it is more susceptible to failure simply because it has more actuators.

Amongst the indices found in literature, the specific resistance is an important dimensionless number used to evaluate the energy efficiency of the mobile robot. It is usually calculated as follows [14]:

$$\varepsilon = \frac{E}{Mgd}, \tag{3}$$

where $E$ is the total energy consumption for traveling the distance $d$, $M$ is the total mass of the robot and $g$ is the gravity acceleration. The second factor of Eq. (2) of the traversability index, as explained in Section 3, evaluates the numbers of steps required to traverse a certain distance. Assuming that, in average, every step requires the same amount of energy, this second factor of the traversability index is actually similar to $\varepsilon$ [14]. The mass of the robot $M$ and the gravity $g$ are taken into account when the simulation is performed.

Furthermore, many authors [3, 14, 15] evaluate the workspace of the robotic leg, assuming that the leg have several DOF independently controlled. A bigger workspace of a leg means that the robot has more possible positions to place its foot in order to reach a stable state. In our case, with one-DOF leg, the workspace of this leg is limited to its predetermined trajectory. The size (length and width) of that trajectory draws a parallel to the workspace of a multiple-DOF leg.

As detailed in Section 3, the developed simulator outputs a traversability index estimating the capability of a leg to cross a certain type of terrain and, as a first approach, this index could be used to optimize the geometric parameters of the legs. However, four additional performance indices are subsequently defined as function of the leg only, without taking into consideration the terrain. This was done in order to obtain an optimal design considering more precisely certain characteristics of the foot trajectory such as smoothness, size and force. The new performance indices were defined to assess the specific problem of optimizing a one-DOF leg.

The traversability index as previously defined indirectly takes into consideration the characteristics of the foot trajectory. However, an optimized leg using only the traversability index could have a good traversability characteristic but its foot trajectory could have rapid changes in direction inducing important torque fluctuations in the joints and actuators, thereby placing an unnecessary burden on the control system. The four additional performance indices proposed in this paper to tackle this issue are defined as follows:

1. Smoothness index: this index reflects the "smoothness" of the foot trajectory produced by the leg. It varies between $(0,1]$ and is calculated as follows:

$$I_{smooth} = \frac{\max\left|\frac{\partial\gamma}{\partial s}\right|}{2\pi}, \tag{4}$$

   where $\gamma$ is the tangent angle to the trajectory and $s$ is the curvilinear abscissa.
   A smooth trajectory obtains a smoothness index close to zero. For example, a circle with a large radius would obtain a smoothness index close to zero. Simply because the change of its tangent angle is constant and equal to the inverse of its radius, once normalized over $2\pi$, would be a value close to zero. Conversely a trajectory with one or several large variations of the tangent angle of the trajectory obtains a smoothness index close to one. The worst case scenario would be a wedge-shaped trajectory where the tangent angle changes very fast.
2. Force index: this index is calculated as the average of the magnitude of the force that the leg is able to apply to the terrain along the support phase, normalized by the maximum value of this force, namely:

$$I_{force} = \frac{\int_0^l |f(s)|\,ds}{l \max|f(s)|}, \tag{5}$$

   this performance index also varies between $(0,1]$. In the above equation, $f$ is the force the leg is able to apply to the terrain during the support phase, $s$ is the curvilinear abscissa of the trajectory and $l$ is the length of the aforementioned support phase. It is desired to maximize this index because the force that the leg is able to apply to the terrain is directly related to the mass it is capable of moving during the support phase.
3. Clearance index: this is defined as the distance between the maximal and minimal points on the ordinate axis of the foot trajectory. The trajectory is defined by two vectors: $\mathbf{x}$ for the abscissa and $\mathbf{y}$ for the ordinate (cf. Fig. 4). The clearance index is normalized by the double of the total length of the leg $(L)$ in order to obtain values between $(0,1]$:

$$I_{clear} = \frac{|\max(\mathbf{y}) - \min(\mathbf{y})|}{2L}, \tag{6}$$

when the clearance index is equal to one, the leg is able to overcome obstacles twice higher than its length.

4. Stride index: this performance index is defined as the distance between the maximal and minimal points on the abscissa axis of the trajectory of the foot (cf. Fig. 4). Similarly to the clearance index, the stride index is also normalized by the double of the total length of the leg ($L$) in order to obtain values between $(0,1]$:

$$I_{stride} = \frac{|\max(\mathbf{x}) - \min(\mathbf{x})|}{2L}, \tag{7}$$

when the stride index is equal to one, the leg is able to traverse a ditch or a low obstacle twice longer than its length.

Using the traversability index obtained from the developed simulator together with the four indices defined above, a combined global performance index may be defined. Different combinations of indices could be made in order to create this global performance index. A set of possible combinations of the four indices depending only on the geometric parameters are:

$$I_{geo} = I_{smooth}, \tag{8}$$

$$I_{geo} = \frac{I_{smooth}}{I_{force}}, \tag{9}$$

$$I_{geo} = \frac{1}{I_{clear} I_{stride}}, \tag{10}$$

$$I_{geo} = \frac{1}{I_{force}}, \tag{11}$$

$$I_{geo} = \frac{1}{I_{clear} I_{stride} I_{force}}. \tag{12}$$

These five combinations were used in the optimization. However, it should be noted that one combinations was discarded. If the smoothness index is combined with the clearance or stride indices, inconsistent results are obtained, as usually, a large trajectory is not smooth and conversely a smooth trajectory is typically small. After the geometric index is calculated, it is combined with the traversability index in order to compute the global performance index, e.g.:

$$I_{global} = \frac{1}{T_{ind}} + I_{geo}. \tag{13}$$

This global performance index was defined as an addition rather than a multiplication similarly to the geometric indices, mainly for practical reasons. At first it was defined as a multiplication, but the global index was a small number and the differences between a good leg and a poorly designed one was even smaller. By defining it as an addition its numeric value is bigger, hence the differences between architecture increases too, which leads to easier reading and analysis of the results. Additionally the optimization algorithm converges faster.

We attempt to develop a mathematical formula that relates the geometric parameters of a leg and the terrain it must traverse with its probability of crossing it. However, due to the non-linearity of the system, this relationship is very difficult to estimate, if not impossible. Because of this, a numerical optimization approach was used instead and yielded good results. The type of optimization performed here is based on a genetic algorithm, a technique well suited to this type of problem as it is capable of finding a solution, even when the analytical method is impractical or cannot yield an exact solution [16].

In our case, the variables to optimize are the geometric parameters of the leg. To achieve this, the function to be optimized performs the traversability simulation presented in Section 3 over a specific terrain, and also computes one of the possible geometric indices to obtain the global performance index. As the main objective of this research is to develop a leg able to cross over different types of terrains, the mean of the traversability index over several types of terrains is used in the optimization. This allows to obtain an optimal architecture for a set of terrains. Several types of terrains, with different sizes of rock filled and gravel surfaces, were selected from the local surroundings. These source terrains were used in the synthetic terrain generation method presented earlier, to become the test grounds for the experimental validation described in Section 6.

## 5 Simulation and optimization of the Chebyshev leg

The Chebyshev leg is one of the most common and oldest architectures for legged robots with one-DOF and it is illustrated in Fig. 5, and described in [17, 18]. Among all one-DOF leg mechanisms found in the literature, the Chebyshev leg was selected as candidate for this prototype mainly for its simple construction and its reduced number of links. Many mobile robots with one-DOF legs use the Chebyshev architecture as a basis to create new leg designs, as presented in [19–22].

The position of the foot of this leg can be calculated using the geometric loop-closure equations, namely:

$$X_p = -c_1 + a_1 \cos\alpha + a_2 \cos\theta, \tag{14}$$

$$Y_p = -a_1 \sin\alpha - a_2 \sin\theta, \tag{15}$$

where $\alpha$ is the actuator angle, $a_1$, $a_2$ and $c_1$ are geometric parameters defining the leg (cf. 5). Finally, the angle $\theta$ is a function of the actuator angle and the geometric parameters, and can be calculated as [23]:

$$\theta = 2\arctan\left(\frac{\sin\alpha - (\sin^2\alpha + A^2 - B^2)}{A+B}\right), \tag{16}$$

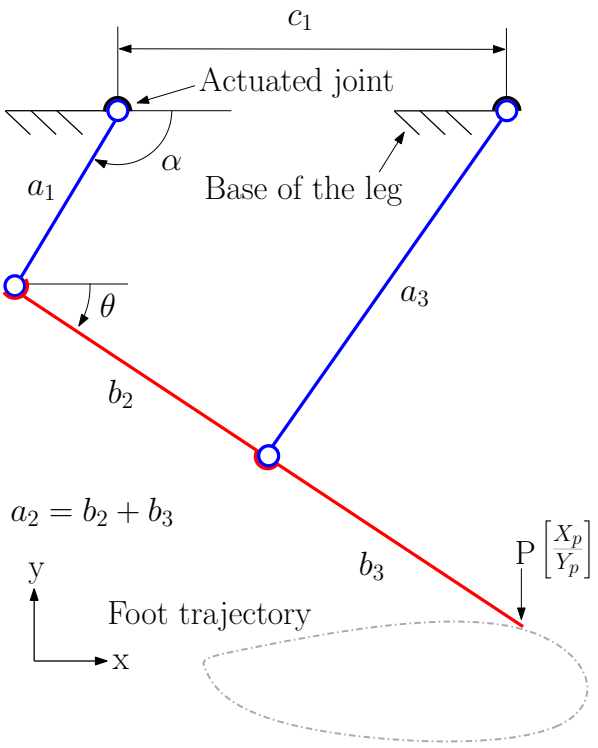


Fig. 5. Chebyshev leg.

where:

$$A = \cos\alpha - \frac{c_1}{a_1}, \tag{17}$$

$$B = \frac{c_1}{b_2}\cos\alpha - \frac{c_1^2 + a_1^2 + b_2^2 - a_3^2}{2a_1b_2}. \tag{18}$$

Afterwards, knowing the Cartesian position of the foot as a function of the actuator angle, the inverse ratio between the displacement of the foot and the angular displacement of the actuator (also known as the mechanical advantage) can be computed, i.e.:

$$R = \frac{\delta\alpha}{\delta s}, \tag{19}$$

where $\delta s$ is the displacement of the foot due to an angular displacement of the actuator $\delta\alpha$ for $\alpha = [0, 2\pi]$. Using the principle of virtual work, to compute the magnitude of the force generated at the foot (in each point of its trajectory) one must multiply the actuator torque $T_a$ (assumed constant) by the previous ratio, i.e.:

$$f = T_a R. \tag{20}$$

With the equations to compute the foot trajectory and the force that the foot is able to apply to the terrain, the geometric parameters of the leg can be optimized in order to obtain the best possible traversability performance for this particular architecture. The total length ($L$) for this leg is defined as $a_3 + b_3$. Additionally, these two lengths were chosen to be constant; $a_3$ was set to 100$[mm]$, and $b_3$ to 86$[mm]$, in order to have the same ratio as the femur and tibia of an average human leg.

Five genetic algorithm optimizations (GA) were performed: one for each possible global performance index described in Eq. (13), depending on which one of the five geometric indices presented in Eqs. (8-12) was used. Each optimization had a population of 100 individuals evolving during 100 generations; the standard Gaussian mutation was used.

In order to obtain a leg able to cross over different types of terrains, these optimizations were repeated over five different types of terrains. These terrains were generated using the terrain generation method detailed in Section 2.

Several digital pictures of different types of uneven terrains were taken to build a library of synthetic terrains. Using the selected leg length (L) as a design parameter, some preliminary optimizations were performed. It was clear that some terrains were impossible to traverse with a leg with the selected length. For the final optimizations the most difficult terrains used were on the limits of the traversing capabilities of any leg with such defined length (L).

Additionally, to obtain an accurate traversability index, the walking process of the leg was simulated over 10 terrains of each type, yielding a total of 50 terrains. The average traversability was finally computed.

Five different sets of geometric parameters corresponding to the five different geometric indices previously defined are obtained. In Fig. 6 the five optimal trajectories are shown, as well as the traversability index of each leg over the most difficult terrain ($I_T$ labels correspond to the $T_{ind}$ expressed in percentage). The origin of the 2D space were the trajectories are represented is the actuated joint of the leg as shown in Fig. 5. The fact that some trajectories obtain a poor traversability index is due to the relative size of the trajectory to the terrain. An example of this is if the standard deviation of the terrain is to big compare to the size of the trajectory the leg.

Table 1. Geometric parameters of optimal legs

| $I_{geo}$ | $c_1[mm]$ | $a_1[mm]$ | $b_2[mm]$ | $T_{ind}[\%]$ |
|---|---|---|---|---|
| $I_{smooth}$ | 115.7 | 14.6 | 53.1 | 93 |
| $\frac{I_{smooth}}{I_{force}}$ | 119.6 | 19.9 | 64.4 | 86 |
| $\frac{1}{I_{clear}I_{stride}}$ | 123.2 | 13.5 | 63.1 | 85 |
| $\frac{1}{I_{force}}$ | 108.2 | 21.0 | 82.1 | 0.8 |
| $\frac{1}{I_{clear}I_{stride}I_{force}}$ | 99.8 | 20.1 | 51.0 | 0 |

The geometric parameters which generated the best tra-

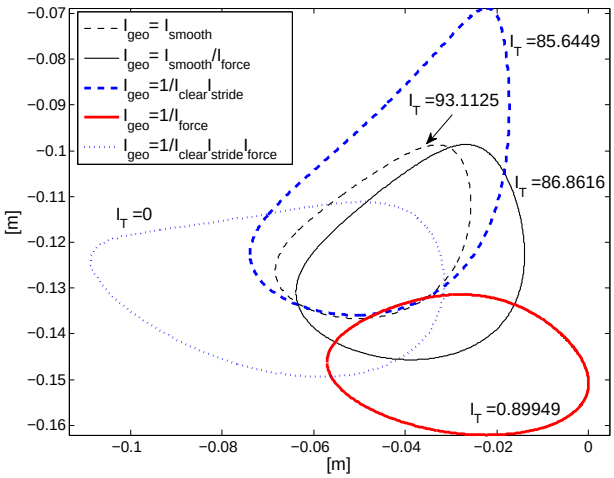


Fig. 6. Trajectories of the Chebyshev leg with optimal geometric parameters.

jectories as well as their traversability index, over the worst terrain, are presented in Table 1. The worst terrain is defined as the terrain where all the legs in average obtained the worst traversability index. These five set of parameters were analyzed and combined to obtain the final geometric parameters that will be used in the prototype with the aim of validating, over a real terrain, the simulation and optimization results. The final lengths are the average of the three legs with the best traversability index. This allows the leg to traverse different types of terrains. For this leg architecture, the lengths obtained are: $c_1 = 119.5[mm]$, $a_1 = 16[mm]$ and $b_2 = 60.2[mm]$.

## 6 Experimental validation and discussions

In order to validate the results obtained from the traversability algorithm developed in this paper, several experiments were performed using a simple walking robot designed for this purpose. The prototype is composed of four legs attached to a frame, as shown in Fig. 7. Each leg is independently actuated by a Maxon F2140 DC brushed 6 Watt motor. All the motors are coupled with a 6:1 GS 38 spur gearbox from the same manufacturer. In addition, a two channel quadrature encoder providing 100 counts per turn is attached to the rear axle of each motor.

The trot gait was chosen to perform the experiments over the real terrains for its simplicity and stability [14]. In this gait the diagonal pairs of legs move in synchrony, with one pair 180° out of phase with respect to the other. A particularity of this gait is that the legs are moving at all times. The legs of the prototype were build using the geometric parameters obtained after performing the optimization described in Section 4.

The final objective is to validate the traversability simulation, with this objective in mind, the lengths used in the prototype were introduced to the simulator and the leg was simulated over different types of terrains. The simulations results are presented in Table 2.

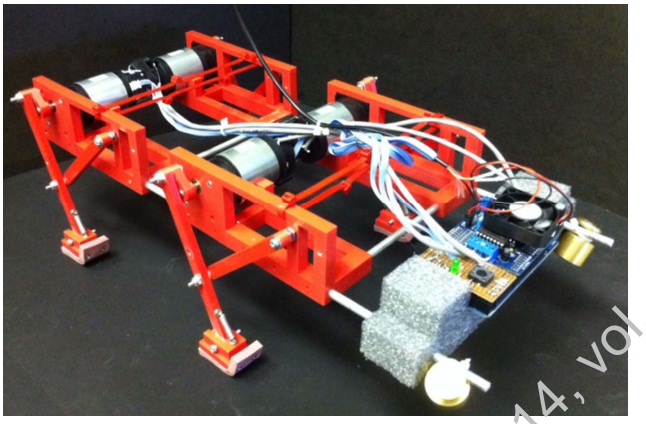

Fig. 7. Robot prototype.

Table 2. Traversability index for different types of terrains

| **Type of terrain** | $T_{ind}$ *Optimal leg* [%] |
|---|---|
| Flat terrain | 94 |
| 11° slope | 87 |
| 18° slope | 82 |
| Sinusoidal terrain | 81 |
| Uneven terrain | 61 |

Using these results as a base line, some real terrains mock-ups were built. In Fig. 8 the simulation of the real prototype leg over a flat terrain, an ascending slope of 11° and a sinusoidal terrain are shown. A stable foothold is represented by the two small consecutive circles. From the latter figure it is clear that the leg is able to traverse the flat terrain with no difficulty. Nevertheless, when it encounters the slope some slippage occurs, this is represented by the thinker dark line. In the case of the sinusoidal terrain a collision occurs in steps number 2 and 6. Additionally, in some steps the leg slipped a greater distance compared with the slope terrain. Although it is not very efficient for this task, the leg is yet again able to traverse the terrain.

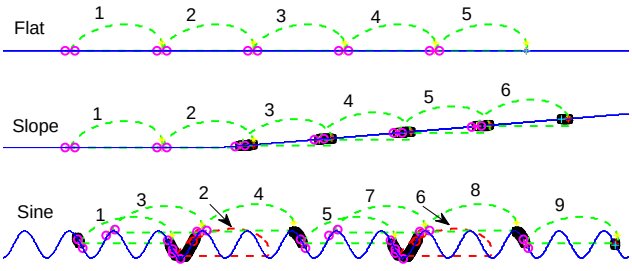


Fig. 8. Simulated foot trajectories over different terrains.

The experiments consisted in making the robot walk over the terrains while being recorded on video. A ruled background was placed behind the robot. Using this back-

ground and knowing the position of the video-camera, the distance that the robot moved over each terrain was determined. Then, the videos were analyzed and the total number of steps that the robot performed was counted. It is important to mention that in the simulation algorithm, the valid and invalid steps, as defined in Section 3, were differentiated. However, in the videos only the total number of steps was considered, as slippage is difficult to establish accurately. Based on these variables a new index was defined as follows:

$$T = \frac{(I_s + V_s)}{D}, \tag{21}$$

where $I_s$ and $V_s$ are the number of invalid and valid steps, $D$ is the distance the robot moved in meters, this new index has $[steps/m]$ as unit. As previously mentioned when analyzing the videos, $(I_s + V_s)$ is simply the total number of steps observed. This index was used to compare the result of the experiments with those of the simulations.

The robot was tested over 5 types of terrains: a flat terrain, an ascending slope of 11° and another one of 18°, a sinusoidal terrain and an uneven terrain composed of river stones. The prototype robot was tried 10 times over each terrain, each time changing randomly the starting point. Then, an average of the index $T$ was computed for each type of terrain. Similarly to the experiments, several simulations were performed for each type of terrain, changing also the starting point, and for each one the index $T$ was computed and finally averaged. The friction coefficient between the foot of the robot and these terrains was measured and input to the simulator. To simulate the traversability of the robot over the uneven aggregation of river stones, the terrain generation method previously developed was used. The results of the simulation and the experiments are shown in Table 3.

Table 3. Experimental and simulation results

| **Type of terrain** | $T_{experimental}$ | $T_{simulation}$ | $\%error$ |
|---|---|---|---|
| Flat terrain | 12.3 | 12.1 | 1.7 |
| 11° slope | 17.1 | 16.4 | 4.3 |
| 18° slope | 22.9 | 21.4 | 7 |
| Sinusoidal terrain | 24.9 | 23.1 | 7.8 |
| Uneven terrain | 22.2 | 21.1 | 5.2 |

As expected, with the flat terrain the simulation and the experimental results are very similar, with less than 2% difference. This result suggests that all the hypothesis and simplifications made by the traversability algorithm for this particular terrain are valid. For the first ascending slope of 11°, the simulation and the experiments differ only by 4.3%, but for the 18° slope the simulation estimated 7% less steps per meter than what was observed in the experiments. This discrepancy is due to the fact that the simulation takes into consideration only one leg, instead of modeling the four legged walking robot used in the experiments. Also, discrepancies were found in the cases of the sinusoidal terrain and the uneven terrain in the results.

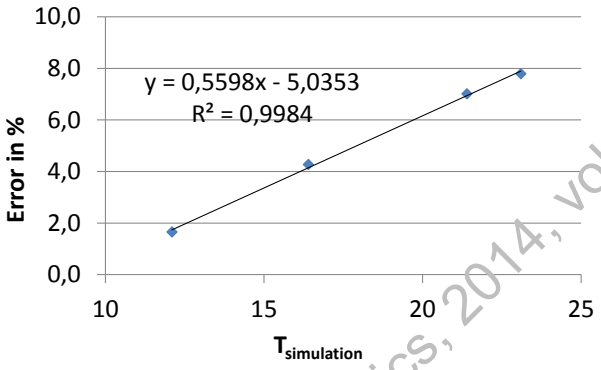


Fig. 9. Error between simulation and experimentation over different terrains.

In Fig. 9 the simulated traversability ($T_{simulation}$), and their corresponding error respect to the experiments, were plotted. To establish a pattern the results of the flat terrain, the two slopes and the sinusoidal terrain were used. A tendency line was added to the graph, showing the quasi-linear relationship between the error and the traversability. The formula of this tendency line was used to formulate a traversability index which takes in consideration the coupling effects between the four legs of the robot. This new index is computed as follows:

$$T_{coupling} = T_{sim} + \frac{(0.56T_{sim} - 5.04)T_{sim}}{100}, \tag{22}$$

where $T_{coupling}$ is the traversability considering the coupling effects and $T_{sim}$ is the traversability of one leg, obtained using the developed simulator. Using this index we obtained traversability for the uneven terrain (whose data was not used to compute Eq. 22) with less than 2% of error when compared with the experimental results.

Fig. 10 shows a series of snapshots from one of the videos where the robot is traversing the uneven terrain. The number in the lower left corner of each snapshot corresponds to the step number. For example, snapshot 1, was taken right before the step number one left the ground and started its swing phase. Step $1-1/2$ corresponds to the moment when the foot landed before it starts to propel the robot forwards. In this experiment the robot also advanced a distance of approximately $30[cm]$ in four steps as in the simulation.

The video also shows occurrences of collisions and slippages. For example, from step 1 to step $1-1/2$ it is apparent that the robot moved backwards as the point where the step $1-1/2$ landed was not stable and the foot slipped. This also occurred between steps 2 and $2-1/2$. Nevertheless, in general, the robot keeps moving forwards. Also, a collision can be observed when step 4 starts leaving the ground and

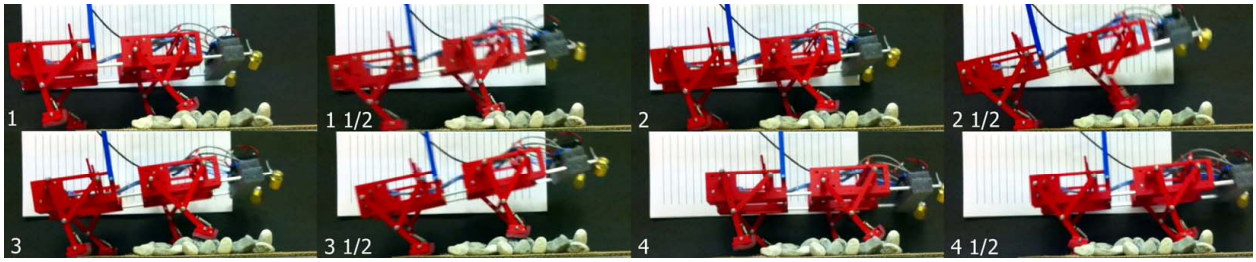


Fig. 10. Snapshots of the robot traversing the uneven terrain.

collides with the terrain. Consequently, step $4-1/2$ landed almost at the same starting point as the take off point.

Using a high speed camera the speed of the robot was measured, it was able to achieved a maximum speed of 1.7 body length per second over a flat terrain. For this measurement the robot used the same trot gait used in all the experiments. Other quadrupeds with multi-DOF like the Tekken or the BigDog obtain similar speeds, of 1.78 and 1.8 body length per seconds [24, 25] respectively. However, the legs of these two robots are driven by three actuators each; hence their failure rate is presumably higher than a leg with fewer DOF.

## 7 Conclusions

In this paper, the authors employed a novel terrain generation method, as well as a traversability simulation algorithm for one-DOF robotic leg architectures. Additionally, new performance indices were introduced to evaluate and optimize this type of mechanisms. In order to validate the traversability simulation, experiments were performed with a legged robot prototype using the Chebyshev leg, one of the most common one-DOF robotic leg architectures. By comparing the results of the experiments and the simulations it can be concluded that the estimation of traversability obtained by the simulation is coherent with the results of the experiments, hence the validity of the newly introduce methodology. The proposed traversability simulations together with the optimization algorithm could help enhance the performances of other one-DOF leg architectures.

## Acknowledgements

The work reported here was performed under a research grant from the Natural Science and Engineering Research of Canada (NSERC). The authors wish to thank Erik Tellier for his help with the mechanical design of the prototype used for the experimental validation. Finally, the support of the Canadian Foundation for Innovation is gratefully acknowledged.

## References

[1] Dwivedi, R., Kandpal, N., and Shukla, A., 2010. "Adaptive suspension system". In Information and Financial Engineering (ICIFE), 2010 2nd IEEE International Conference, pp. 694–697.

[2] Kilit, O., and Yontar, A., 2009. "Stability of a new mars rover with multi-stage bogie mechanism". In Recent Advances in Space Technologies, 2009. RAST '09. 4th International Conference, pp. 145–149.

[3] Loc, V.-G., Koo, I. M., Trong, T., Kim, H. M., Moon, H., Park, S., and Choi, H. R., 2010. "A study on traversability of quadruped robot in rough terrain". In International Conference on Control Automation and Systems (ICCAS), pp. 1707–1711.

[4] Remy, C. D., Baur, C., Latta, M., Lauber, A., Hutter, M., A, M., Hoepflinger, Pradalier, C., and Siegwart, R., 2010. "Walking and crawling with alof: a robot for autonomous locomotion on four legs". In Proceedings of CLAWARD'2010: 13th International Conferece on Climbing and Walking Robots and the Support Technologies for Mobile Machines, Vol. 38, pp. 264–268.

[5] Amagata, Y., Nakaura, S., and Sampei, M., 2008. "The running of humanoid robot on uneven terrain utilizing output zeroing". In SICE Annual Conference, Technische Universiteit Eindhoven, pp. 2841–2846.

[6] Gibbesch, A., and Schafer, B., 2005. "Multibody system modeling and simulation of planetary rover mobility on soft terrain". In The 8th International Symposium on Artifical Intelligence, Robotics and Automation in Space - iSAIRAS.

[7] Gu, J., Cao, Q., and Huang, Y., 2008. "Rapid traversability assessment in 2.5d grid-based map on rough terrain". *International Journal of Advanced Robotic Systems,* **5**(4), pp. 389–394.

[8] Li, W., Huang, Y., Cui, Y., Dong, S., and Wang, J., 2010. "Trafficability analysis of lunar mare terrain by means of the discrete element method for wheeled rover locomotion". *Journal of Terramechanics,* **47**(3), pp. 161–172.

[9] Palmer, L., and Orin, D., 2007. "Quadrupedal running at high speed over uneven terrain". In Intelligent Robots and Systems, 2007. IROS 2007. IEEE/RSJ International Conference on, pp. 303–308.

[10] Yokokohji, Y., Chaen, S., and Yoshikawa, T., 2004. "Evaluation of traversability of wheeled mobile robots on uneven terrains by fractal terrain model". In Proceedings. ICRA '04. IEEE International Conference on Robotics and Automation, Vol. 3, pp. 2183–2188.

[11] Deussen, O., and Lintermann, B., 2005. *Digital Design of Nature Computer Generated Plants and Organics*. X.media.publishing, ch. Modeling Terrain, pp. 113–

123.

[12] Ruella, C., and Birglen, L., 2013. "Traversability analysis of a novel one-dof robotic leg". In Proceedings of the 2013 ASME International Design Engineering Technical Conferences and Computers and Information in Engineering Conference (IDETC-CIE).

[13] Spong, M. W., Hutchinson, S., and Vidyasagar, M., 2005. *Robot Modeling and Control*. John Wiley & Sons, Inc.

[14] Kajita, S., and Espiau, B., 2008. *Handbook of Robotics*. Springer, Berlin-Heidelberg, ch. Legged Robots, pp. 361–389.

[15] Hirose, S., Fukuda, Y., Yoneda, K., Nagakubo, A., Tsukagoshi, H., Arikawa, K., Endo, G., Doi, T., and Hodoshima, R., June 2009. "Quadruped walking robots at tokyo institute of technology". *Robotics & Automation Magazine, IEEE,* **Vol.16, no.2,**, pp. pp.104–114.

[16] Whitley, D., 1994. *A Genetic Algorithm Tutorial*, samizdat press ed. Computer Science Department, Colorado State University, Fort Collins, Co 80523.

[17] Artobolevsky, I., 1989. *Mechanisms in modern engineering design*, Vol. I-III. MIR Publisher Moscow.

[18] Raibert, M. H., 1986. "Legged robots". *Communications of the ACM,* **29**(6), pp. 499–514.

[19] Tavolieri, C., Ottaviano, E., Ceccarelli, M., and Rienzo, A. D., 2006. "Analysis and design of a 1-dof leg for walking machines". In The 15th International Workshop on Robotics in Alpe-Adria-Danube Region (RAAD).

[20] Shieh, W., Tasai, L., and Azarm, U., 1997. "Design and optimization of a one-degree-of-freedom six-bar leg mechanism for a walking machine". *Journal of Robotics systems,* **14**(12), pp. 871–880.

[21] Kendry, J. M., 2008. "Design and analysis of a class of planar biped robots mechanically coordinated by a single degree of freedom". *ASME Journal of Mechanical Design,* **130**, p. 102302.

[22] Tavolieri, C., Ottaviano, E., Ceccarelli, M., and Rienzo, A. D., 2007. "A design of a new leg-wheel walking robot". In Mediterranean Conference on Control & Automation.

[23] Ottaviano, E., Lanni, C., and Ceccarelli, M., 2004. "Numerical and experimental analysis of a pantograph-leg with a fully-rotative actuating mechanism". In Proceedings of the 11th World Congress in Mechanism and Machine Science, pp. 1537–1541.

[24] Fukuoka, Y., and Kimura, H., 2009. "Dynamic locomotion of a biomorphic quadruped tekken robot using various gaits: walk, trot, free-gait and bound". *Applied Bionics and Biomechanics,* **6:1**, pp. 63–71.

[25] Raibert, M., Blankespoor, K., Nelson, G., and Playter, R., 2008. "Bigdog, the rough-terrain quadruped robot". In Proceedings of the 17th World CongressThe International Federation of Automatic Control.